

Interactive comment on “Bayesian approach for three-dimensional aquifer characterization at the hanford 300 area” by H. Murakami et al.

H. Murakami et al.

harukom@nuc.berkeley.edu

Received and published: 9 September 2010

We appreciate the constructive comments. The responses to the comments are as follows. Four figures (Fig. C1-1 to Fig. C1-4) were added at the end of this document.

Response to Comment Number 4:

In terms of increasing information, we will respond in Response to Specific Comments 4.

Full Screen / Esc

Printer-friendly Version

Interactive Discussion

Discussion Paper



Response to Comment Number 10:

We added "2-D" at the following locations to state "2-D T field" or "2-D geostatistical parameters"; P2023-L3, P2030- L17, P2032- L4, P2032- L5, P2032-L18, P2033-L21, P2033- L22, P2033-L26, P2035-L14, P2035-L16, P2035-L25.

Response to Comment Number 13:

Regarding the posterior distributions, we will respond in Response to Specific Comments 4. The 3-D mean field is shown in Fig. C1-1. We can see the high-low-high layers in $\ln K$ along the centerline, which is consistent with the observations in the tracer tests later conducted at the site (Rockhold et.al., 2010; Zachara, 2010).

Response to Specific Comment Number 1:

Corrected.

Response to Specific Comment Number 2:

It is true that we use the current estimate of the T field in the sensitivity analysis. Before the injection test, however, we do not have any local information on the T field, since our priors are only for the global parameters (i.e., mean, variance, and scale). This leads to the prior estimate of the T field being uniform over the domain. When we solve the sensitivity equation for a flat transmissivity field, the sensitivity is high around

Full Screen / Esc

Printer-friendly Version

Interactive Discussion

Discussion Paper



observation wells, which is consistent with previous studies by Castagna and Bellin (2009) and Vasco et al. (2000).

In response to the comment that "focusing anchors at observation point locations might lead to overfitting or point calibration," we would refer to Rubin et al. (2010), now in press and available on the website of Water Resources Research, for more detailed discussions. Overfitting occurs in optimization or fitting procedures as reported with using other inverse modeling methods. In MAD, the anchor values are inferred as a joint distribution without fitting procedures. MAD therefore does not incur overfitting problems.

Response to Specific Comment Number 3:

As epistemic errors, i.e., errors due to lack of knowledge arising from simplified models (Rubin, 2003), we may consider errors due to 2-D flow approximations, well construction, and other unknown errors during the injection tests. We assume that those epistemic errors are negligible, since we thoroughly examined the 2-D flow assumption in Section 3, and the wells were carefully constructed to minimize any artifacts (Bjornstad et al., 2009). For quantifying the errors, we followed Nowak et al. (2005) and Li et al. (2008), who determined the errors based on fluctuation or noise in the pressure measurements. In our case, the noise is contained within the range of the instrument resolution.

Response to Specific Comment Number 4:

Although we may expect tighter distributions with more information, some of the uncertainty cannot be eliminated due to measurement errors and the limited number of

Full Screen / Esc

Printer-friendly Version

Interactive Discussion

Discussion Paper



observation wells. In addition, the same observation wells were used repeatedly for several tests. Zhu and Yeh (2005) and Yeh and Li (2000) also reported that increasing the number of pumping tests does not improve the estimation above a certain number (three to four tests in their cases).

We have added three additional tests in the synthetic study. We revised the injection-test configuration in Fig. 2 as Fig. C1-2. Figure C1-3 shows the change in the marginal posterior distributions with increasing numbers of injection tests. We added a 5-test case (Well 2-09, 2-11, 2-18, 2-24 and 3-24), a 6-test case (Well 2-09, 2-11, 2-16, 2-18, 2-24 and 3-24) and a 7-test case (Well 2-09, 2-11, 2-16, 2-18, 2-19, 2-24 and 3-24). Although the distribution for variance was improved slightly compared to the 4-test case, the improvement from increasing the number of tests more than 4 tests is not significant.

Response to Specific Comment Number 5:

We added five realizations of transects, shown in Fig. C1-4. In Fig. C1-4 (b), which is based on the three tests, we can see that all the generated fields have a transition from high to low $\ln K$ near the center along the true field. The anchors capture this feature. Without anchors, it would be impossible to capture such local heterogeneity, since the mean field would be flat with the global mean value.

Additional References

Bjornstad, B. N., Horner, J. A., Vermuel, V. R., Lanigan, D. C., and Thorne, P. D.: Borehole completion and conceptual hydrogeologic model for the IFRC Well Field, 300 Area, Hanford Site PNNL-18340, Pacific Northwest National Laboratory, Richland,

Washington, 2009.

Li, W., Englert, A., Cirpka, O. A., and Vereecken, H.: Three-dimensional geostatistical inversion of flowmeter and pumping test data, *Ground Water*, 46(2), 193–201, 2008.

Nowak, W., and Cirpka, O.A: Geostatistical inference of hydraulic conductivity and dispersivities from hydraulic heads and tracer data, *Water Resour. Res.*, 42, W08416, doi:10.1029/2005WR004832, 2006.

Yeh, T.-C. J., and Liu, S.: Hydraulic tomography: Development of a new aquifer test method, *Water Resour. Res.*, 36(8), 2095– 2105, 2000.

Zachara J.M.: Annual Report to the DOE Office of Science, Climate and Environmental Sciences Division (January 2009 to January 2010), Multi-Scale Mass Transfer Processes Controlling Natural Attenuation and Engineered Remediation: An IFRC Focused on Hanford's 300 Area Uranium Plume. PNNL-19209, Pacific Northwest National Laboratory, Richland Washington, 2010.

Zhu, J., and Yeh, T.-C. J.: Characterization of aquifer heterogeneity using transient hydraulic tomography, *Water Resour. Res.*, 41, W07028, doi:10.1029/2004WR003790, 2005.

Complete Figure Captions

* Due to the limited space, the caption below each figure is truncated.

Figure C1-1. 3-D mean $\ln K$ field in the saturated portion of the Hanford formation. The black dots and lines represent the well locations. The reference point of local coordinates is at (594 164 m, 115 976 m) in the Hanford coordinates.

Figure C1-2. Configuration of injection and observation wells in each test. The reference point of local coordinates is at (594 164 m, 115 976 m) in the Hanford coordinates.

Full Screen / Esc

Printer-friendly Version

Interactive Discussion

Discussion Paper



Figure C1-3. Marginal posterior distributions of the structural parameters (mean, variance, and scale) in the synthetic study, with their corresponding true values. The distributions based on the different number of tests are compared.

Figure C1-4. Comparison among the reference field, the mean field, and the 98% confidence interval of the generated fields, along the center line of the IFRC well field (Line A-B in Fig. 4), for the inversion based on (a) one test (injection at Well 2-18) and (b) three tests (injections at Wells 2-09, 2-24, and 3-24). The gray lines are the realizations of the fields.

Interactive comment on Hydrol. Earth Syst. Sci. Discuss., 7, 2017, 2010.

Full Screen / Esc

Printer-friendly Version

Interactive Discussion

Discussion Paper



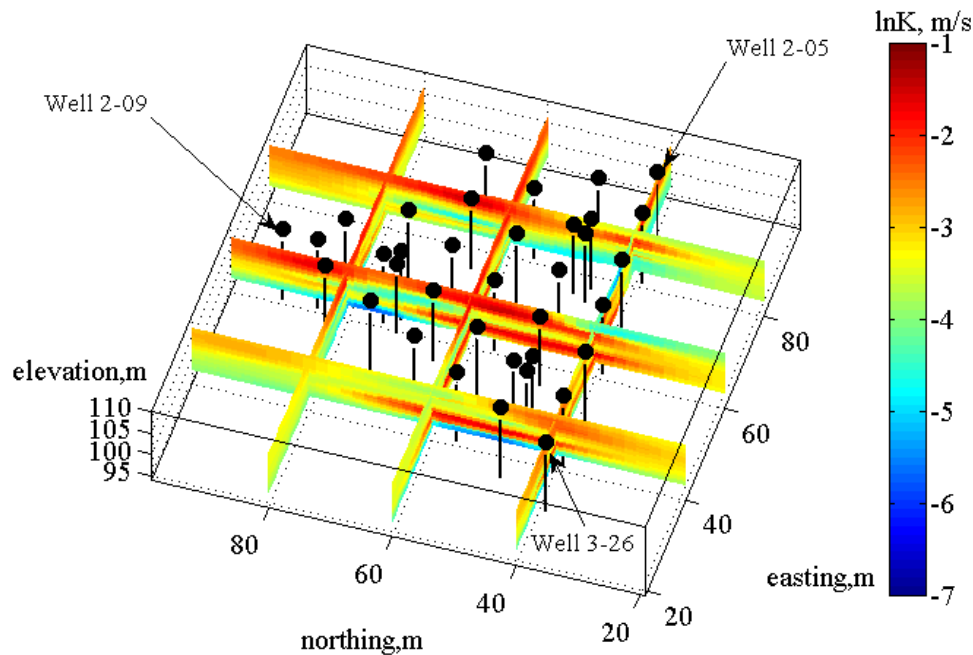


Fig. 1. (Figure C1-1). 3-D mean $\ln K$ field in the saturated portion of the Hanford formation. The black dots and lines represent the well locations. The reference point of local coordinates is at (594 164 m, 1

Interactive
Comment

Full Screen / Esc

Printer-friendly Version

Interactive Discussion

Discussion Paper



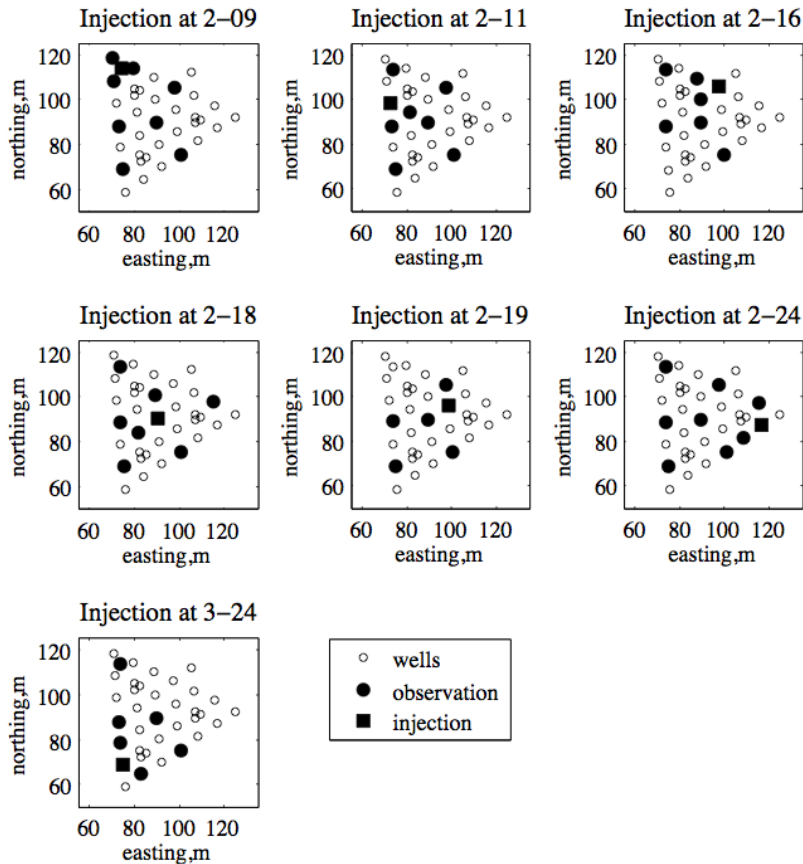


Fig. 2. (Figure C1-2). Configuration of injection and observation wells in each test. The reference point of local coordinates is at (594 164 m, 115 976 m) in the Hanford coordinates.

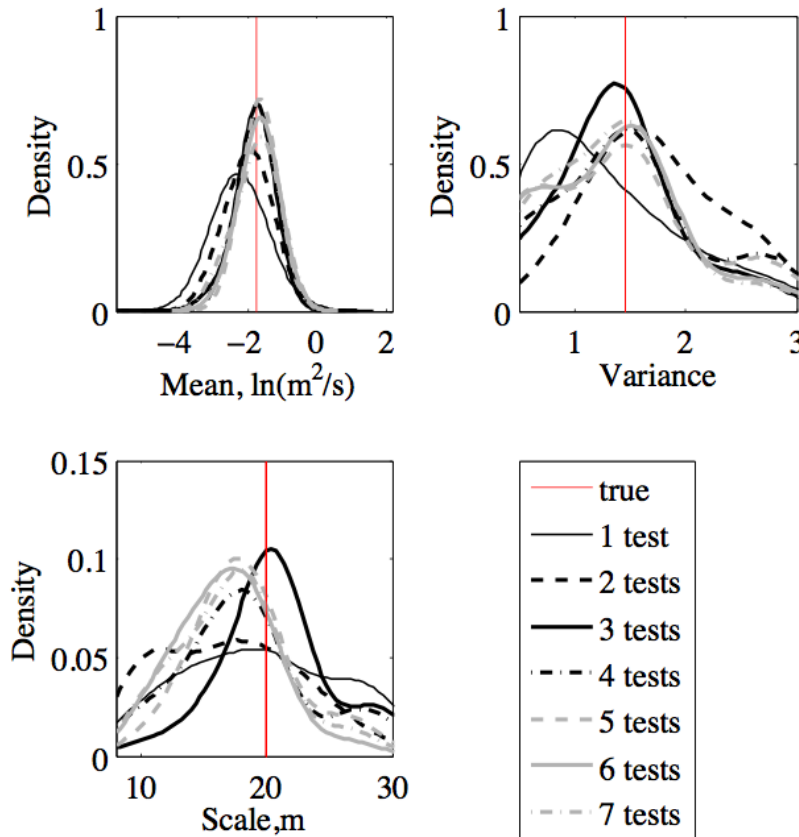
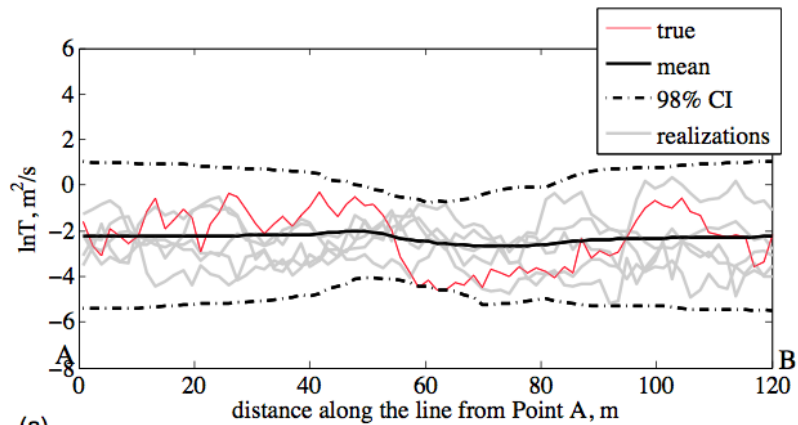
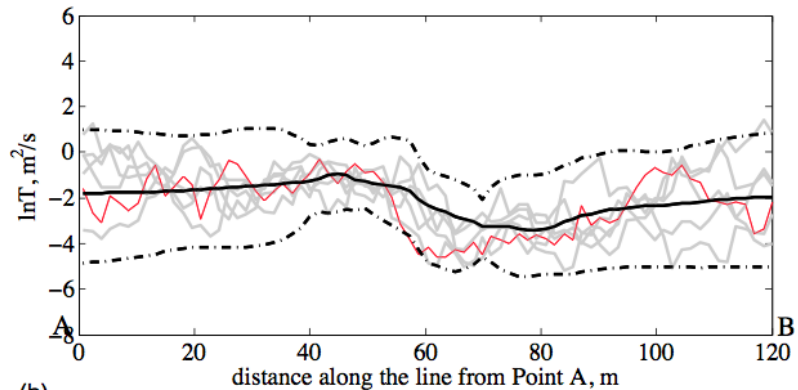


Fig. 3. (Figure C1-3). Marginal posterior distributions of the structural parameters (mean, variance, and scale) in the synthetic study, with their corresponding true values. The distributions based on the di



(a)



(b)

Fig. 4. (Figure C1-4). Comparison among the reference field, the mean field, and the 98% confidence interval of the generated fields, along the center line of the IFRC well field (Line A-B in Fig. 4), for th